NUREG/CR-3644
LA-10007-MS

Los Alamos National Laboratory is operated by the University of California for the United States Department of Energy under contract W-7405-ENG-36.

Review of Proposed Failure Criteria for Ductile Materials

Los Alamos National Laboratory
Los Alamos, New Mexico 87545

GPO Printed copy price: $3.75

NUREG/CR-3644
LA-10007-MS

R7

Review of Proposed Failure Criteria for Ductile Materials

Frederick D. Ju*
Thomas A. Butler

Manuscript submitted: January 1984
Date published: April 1984

Prepared for
Clinch River Breeder Reactor Program Office
Office of Nuclear Reactor Regulation
US Nuclear Regulatory Commission
Washington, DC 20555

NRC FIN No. A7270

*Collaborator at Los Alamos. Mechanical Engineering Department, University of New Mexico, Albuquerque, NM 75131.

Los Alamos National Laboratory
Los Alamos, New Mexico 87545

CONTENTS

ABSTRACT. 1

I. INTRODUCTION 1

II. PLASTIC YIELD CRITERIA 2

III. THEORIES OF DUCTILE FRACTURE 7

IV. GENERAL REVIEW 19

REFERENCES. 27

FIGURES

1. Envelope of Mohr's stress plane. 3

2. Comparison of Tresca-Mohr's and Hencky-Mises' yield criteria. Reprinted with permission from An Introduction to the Mechanics of Solids, S. H. Crandall and N. C. Dahl, copyright 1959, McGraw-Hill Book Co. 5

3. Growing normal fracture and incipient delaminating and shear fractures in necked copper tensile specimen. Reprinted with permission from Fracture, F. A. McClintock, "Plastic Aspects of Fracture," copyright 1971, Academic Press. 8

4. Equivalent and engineering flow stress-strain curves in tension and compression for AISI 1020 steel, hot-rolled. Reprinted with permission from An Introduction to the Mechanics of Solids, S. H. Crandall and N. C. Dahl, copyright 1959, McGraw-Hill Book Co. . . . 10

5a. Ramberg-Osgood $\bar{\sigma}$ - $\bar{\varepsilon}$ curve ($\bar{\sigma} = A\bar{\varepsilon}^n$) based on maximum strain $\varepsilon_f = 0.7$ for AISI 1020 steel. 12

5b. Ramberg-Osgood models ($\bar{\sigma} = A\bar{\varepsilon}^n$) for AISI 1020 steel for equal stability point. 12

6. Critical subtangent to the generalized strain-hardening curve. 15

7. Coalescence of holes. McClintock (1968). Reprinted with permission from Journal of Applied Mechanics, F. A. McClintock, "A Criterion for Ductile Fracture by the Growth of Holes," copyright 1968, American Society of Mechanical Engineers. 16

8. Strain plane with corresponding deformations of a cube containing two holes coalescing in the b direction. Reprinted with permission from Journal of Applied Mechanics, F. A. McClintock, "A Criterion for Ductile Fracture by the Growth of Holes," copyright 1968, American Society of Mechanical Engineers. 17

9. Comparison of ductility of copper-dispersion alloys with hole-growth theory. Reprinted with permission from Ductility, F. A. McClintock, "On the Mechanics of Fracture from Inclusions," copyright 1968, American Society for Metals. 18

10. The major principal stress circles representing the stresses at fracture in Bridgman's tension tests for steel bars exposed simultaneously to high hydrostatic pressure p. Reprinted with permission from Theory of Flow and Fracture of Solids, A. Nadia, copyright 1950, McGraw-Hill Book Co. 20

11. Correlation between fracture strain and ratio of hydrostatic pressure to effective stress at fracture. Reprinted with permission from Ductility, G. E. Dieter, "Introduction to Ductility," copyright 1968, American Society for Metals. 21

12. Effect of biaxial stress state on ductility of sheet steel. Reprinted with permission from Ductility, G. E. Dieter, "Introduction to Ductility," copyright 1968, American Society for Metals. 22

13. Comparison of damage for exact and approximate equations of hole-growth theory 23

14. Fracture strain as a function of triaxiality factor. 24

15. Fracture criterion proposed by Westinghouse. 25

REVIEW OF PROPOSED FAILURE CRITERIA FOR DUCTILE MATERIALS

by

Frederick D. Ju and Thomas A. Butler

ABSTRACT

In this report, failure criteria for structural components constituting the primary coolant-system boundary of a Liquid Metal Fast Breeder Reactor (LMFBR) are reviewed. Because the materials being considered, mild ferritic steel and austenitic stainless steels, are ductile, especially under LMFBR normal operating and accident conditions, only ductile criteria are considered. The ductile criteria must be used in combination with true stress and strain measures of deformation and internal load. Specific criteria reviewed include maximum stress and strain or plastic instability based on uniaxial tensile-test data and a hole-growth theory based on coalescence of neighboring voids under load. Criteria based only on maximum stress or strain are not recommended for general use because they are not appropriate under general, multiaxial stress conditions. The plastic instability criterion, because it leaves a large unused toughness region before fracture, is recommended where considerable conservatism is warranted. The hole-growth criterion is recognized as being analytically sound; however, it has not been extended to general three-dimensional geometry and multiaxial stress conditions. The theory needs to be substantiated with experimental data for specific materials being considered.

I. INTRODUCTION

The purpose of this report is to review material-failure criteria that are being used to evaluate Clinch River Breeder Reactor (CRBR) structural response to accident loadings. Because of the nature of the materials being considered and the environment to which they are submitted, we consider only ductile failure criteria.

The ductile materials will have an approximately linear elastic range and a large-strain, nonlinear, work-hardening range: typical materials are mild

steel and austenitic stainless steel. Materials in the same classification may not have similar crystalline structures. Whereas brittle fracture is the single failure phenomenon for brittle materials, ductile materials may, depending upon the level of service limits, have either elastic limits or ductile fracture as the material-failure criteria. For ductile fracture, no relatively simple criterion exists for computational use.

Fracture criteria are inevitably related to stresses and strains. For yield criteria, because of the small deformation, both the stress and the strain measures normally refer to the undeformed geometry--the initial cross-sectional area and the initial gauge length. Such measures are called the engineering definitions of stress and strain. In ductile fracture, where large deformations are generally the rule, the deformed cross-sectional area can be much different from the original undeformed area. Therefore, the "true" stress on the deformed area is normally used. It is reasonable to define, for the purpose of ductile fracture-initiation analysis, both the stress and the strain measures in terms of the current deformed geometry. The differences can be quite different from those using engineering definitions, both in terms of magnitudes and constitutive relationships. True stresses and true strains will be treated further in the section on ductile fracture.

II. PLASTIC YIELD CRITERIA

Under static or quasi-static loading, materials reach the elastic-failure limit by yielding plastically; the failure criteria are, therefore, the criteria for plastic yielding. Currently either Tresca-Mohr's maximum-shearing-stress theorem or the Hencky-Mises energy-of-distortion theorem[1] is used to define the yield surface. The modified maximum-shearing-stress theorem can be expressed in terms of the maximum and the minimum principal stresses (σ_1 and σ_3),

$$| \sigma_1 - \sigma_3 | = f(\sigma_1 + \sigma_3) \quad . \tag{1}$$

Equation (1) defines an envelope in the Mohr's stress plane, Fig. 1. The given function is usually assumed constant for materials with similar tensile and

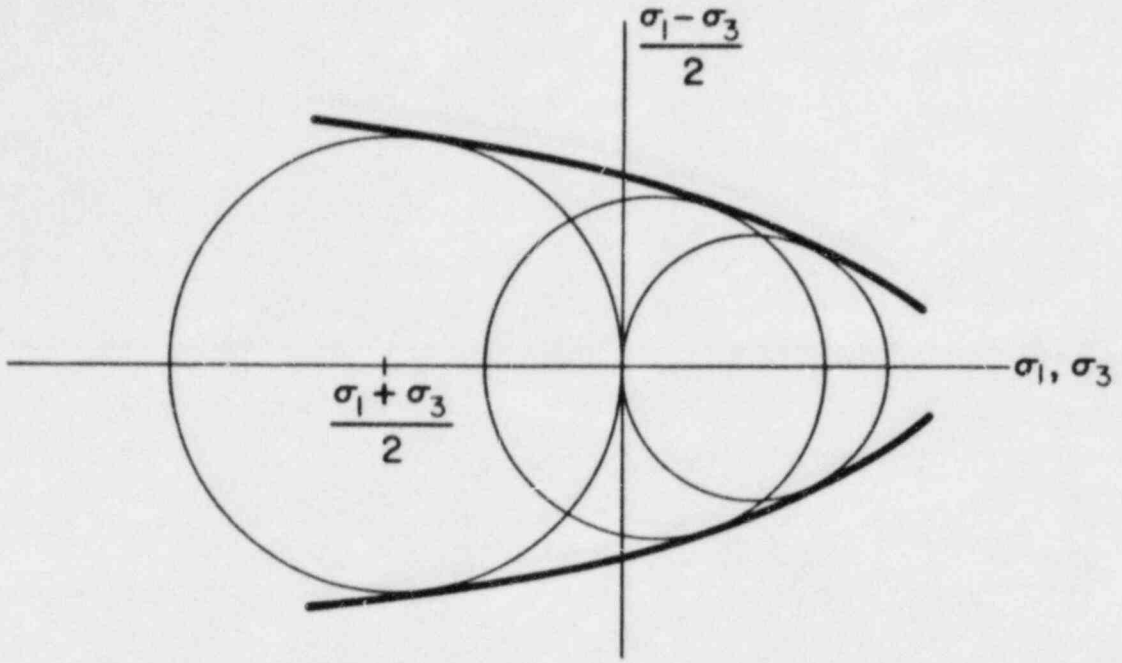

Fig. 1. Envelope of Mohr's stress plane.

compressive elastic properties. The intermediate principal stress is noticeably not included in the criterion. This fact constitutes one of the major criticisms of the criterion, although it is generally considered a more conservative criterion than the energy-of-distortion theorem.

The general expression for Hencky-Mises theorem is

$$J_2' = f(p), \tag{2}$$

where J_2' is the second invariant of stress deviator (s_{ij}) and p is the local hydrostatic pressure. Copper, aluminum, and, to some extent, steel are not affected by the local pressure. For those materials, the Hencky-Mises yielding criterion [Eq. (2)] becomes

$$J_2' = \text{constant} = k^2 . \tag{3}$$

Figure 2 compares criteria of Eq. (1) and Eq. (2), when the limit functions, f, have corresponding constants at yield based on uniaxial experiments. In

Fig. 2a some experimental data are superposed, indicating the closer prediction by the Hencky-Mises criterion. Several theories that originated from or are related to the Hencky-Mises theorem and that are based on uniaxial tensile experiments are given below.

Hencky-Mises Yielding Condition

When the Hencky-Mises condition relates the constant k^2 to the uniaxial tension experiment, Eq. (3) becomes

$$J_2' = \frac{1}{6}\left[(\sigma_1 - \sigma_2)^2 + (\sigma_2 - \sigma_3)^2 + (\sigma_3 - \sigma_1)^2\right] = \frac{1}{3}\sigma_y^2 , \tag{4}$$

where σ_y is the tensile yield stress.

Principle of Energy-of-Distortion

The principle predicts yielding when the energy-of-distortion reaches a limiting value determined by a uniaxial tension experiment. Here

$$U_d = \frac{1}{2} s_{ij} e_{ij} = \frac{1}{4\mu} s_{ij} s_{ij} = U_e - U_{\text{hydrostatic}} , \tag{5}$$

where $\{s_{ij}\}$ and $\{e_{ij}\}$ are the stress and strain deviators respectively, U_e is the strain energy, and $U_{\text{hydrostatic}}$ is that portion of the strain energy in hydrostatic deformation. Hence, the energy-of-distortion in uniaxial tension is

$$U_d\Big|_{\text{uniaxial}} = \frac{1}{6\mu}\sigma^2 . \tag{6}$$

The principle reinforces the Hencky-Mises condition that

$$J_2' = \frac{1}{2} s_{ij} s_{ij} = \frac{1}{3}\sigma_y^2 .$$

Octahedral Stress Criterion

Define an octahedral plane, with unit normals of $(1/\sqrt{3}, 1/\sqrt{3}, 1/\sqrt{3})$ in principal coordinates of the stress tensor. Then the octahedral stress criterion states that yielding initiates when the shearing stress on that plane

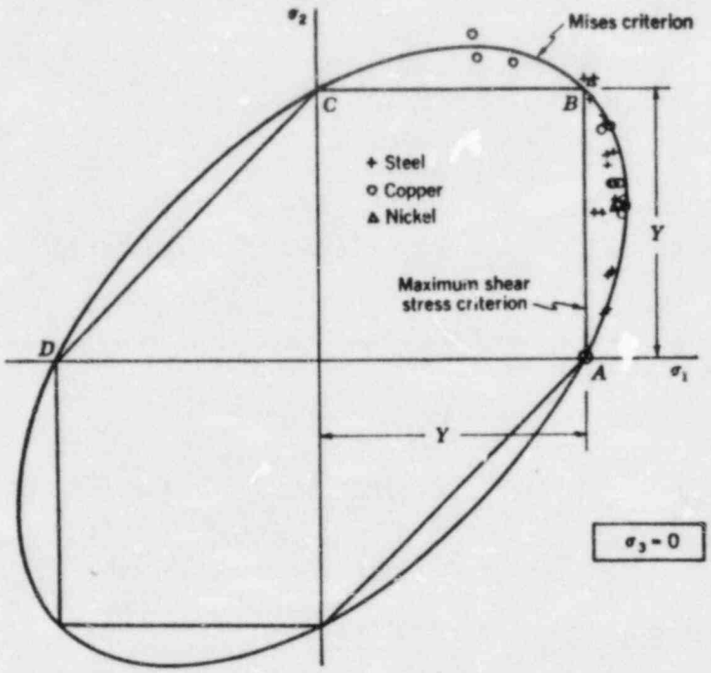

(a) Two-dimensional stress state.

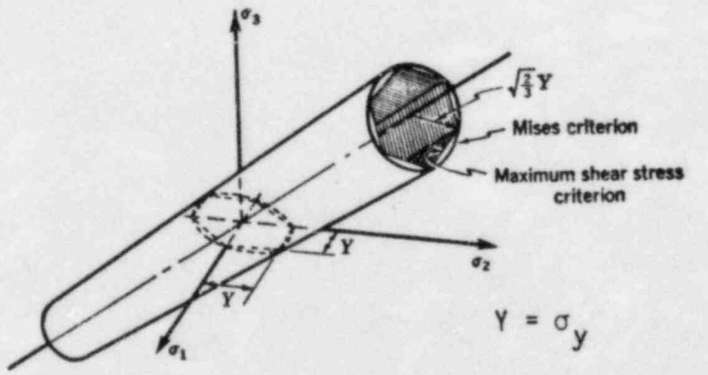

(b) Three-dimensional stress state.

Fig. 2. Comparison of Tresca-Mohr's and Hencky-Mises' yield criteria. Reprinted with permission from An Introduction to the Mechanics of Solids, S. H. Crandall and N. C. Dahl, copyright 1959, McGraw-Hill Book Co.[2]

reaches a limit, which is determined by the uniaxial tension experiment. The octahedral shearing stress can be readily determined as

$$\sigma_{\tau'oct} = \frac{1}{3}\sqrt{(\sigma_1 - \sigma_2)^2 + (\sigma_2 - \sigma_3)^2 + (\sigma_3 - \sigma_1)^2} = \sqrt{\frac{2}{3} J_2'} . \qquad (7)$$

The octahedral shearing stress for uniaxial tension is then

$$\sigma_{\tau}\Big|_{\text{oct-ten}} = \frac{\sqrt{2}}{3}\,\sigma . \qquad (7a)$$

The limit is reached when $\sigma = \sigma_y$. Then Eqs. (7) and (7a) become equivalent to Eq. (4).

Equivalent Stresses and Equivalent Strains

The concept introduces an artificial uniaxial stress (or strain) equivalent to a complex triaxial stress (or strain) state, such that [see Eq. (4)]

$$\sigma_e = \sqrt{\frac{1}{2}[(\sigma_1 - \sigma_2)^2 + (\sigma_2 - \sigma_3)^2 + (\sigma_3 - \sigma_1)^2]} = \sqrt{3J_2'} = \frac{3}{\sqrt{2}}\,\sigma_t\Big|_{oct} \qquad (8)$$

or

$$\varepsilon_e = \frac{1}{1+\nu}\sqrt{\frac{1}{2}[(\varepsilon_1 - \varepsilon_2)^2 + (\varepsilon_2 - \varepsilon_3)^2 + (\varepsilon_3 - \varepsilon_1)^2]} , \qquad (9)$$

for engineering definitions of stress and strain. The limits for these criteria are the yield strength (σ_y) and the yield strain (ε_y), respectively. For the true stress and true strain the equivalent stress and strain are defined as

$$\bar{\sigma}_e = \sqrt{3J_2'} = \sqrt{\frac{1}{2}[(\bar{\sigma}_1 - \bar{\sigma}_2)^2 + (\bar{\sigma}_2 - \bar{\sigma}_3)^2 + (\bar{\sigma}_3 - \bar{\sigma}_1)^2]} \qquad (8a)$$

and

$$\bar{\varepsilon}_e = \frac{1}{3}\sqrt{2[(\bar{\varepsilon}_1 - \bar{\varepsilon}_2)^2 + (\bar{\varepsilon}_2 - \bar{\varepsilon}_3)^2 + (\bar{\varepsilon}_3 - \bar{\varepsilon}_1)^2]} . \qquad (9a)$$

The quantities $\bar{\sigma}_i$ and $\bar{\epsilon}_i$ are the principal values of true stress and strain, which are defined in Sec. III.

Although the above-stated criteria seem to generate the same yield condition, some physical interpretation differences do exist. The Hencky-Mises condition and the octahedral shearing-stress criterion are both controlled by the state of stress only. The energy-of-distortion principle is also governed to a certain extent by the constitutive relationship: the equivalent stress and strain are both artificial; the former is less physically meaningful than the octahedral shearing stress; the latter is meaningful in linear elastic materials only. Furthermore, the equivalence of all these criteria is based on the linear constitutive equations with small deformation. Extension to large deformation must be justified on individual cases of loading and deformation.

III. THEORIES OF DUCTILE FRACTURE

Ductile fracture is a general term to describe fracture that is preceded by relatively large plastic deformation in the neighborhood of the fracture zone. It is distinguished from the term rupture in the present-day usage. Theoretically, the latter is restricted to a phenomenon in which the cross-sectional area at rupture is reduced practically to zero. Ductile fractures occur in the form of normal cracking, delamination, fracture in the shear band, or, most likely, a combination of all of these (Fig. 3). Fracture initiation and mode of fracture are governed by many factors, principally by the current state of stress, the entire course of straining, and the history of loading for a specific material. Theories of fracture initiation should individually address criteria for specific modes of fracture in specific crystalline structures. It is doubtful that there exists a single limiting value that is applicable to all cases of failure analyses.

In establishing a limiting value for a specific failure criterion, most theories refer to the data derived from uniaxial experiments. The generally available mechanical properties of materials are the yield stress and the yield strain, the ultimate strength, and the maximum elongation, all in the engineering definitions. The yield stress and the yield strain (σ_y, ϵ_y) define a single point on the engineering stress-strain curve marking the start of the

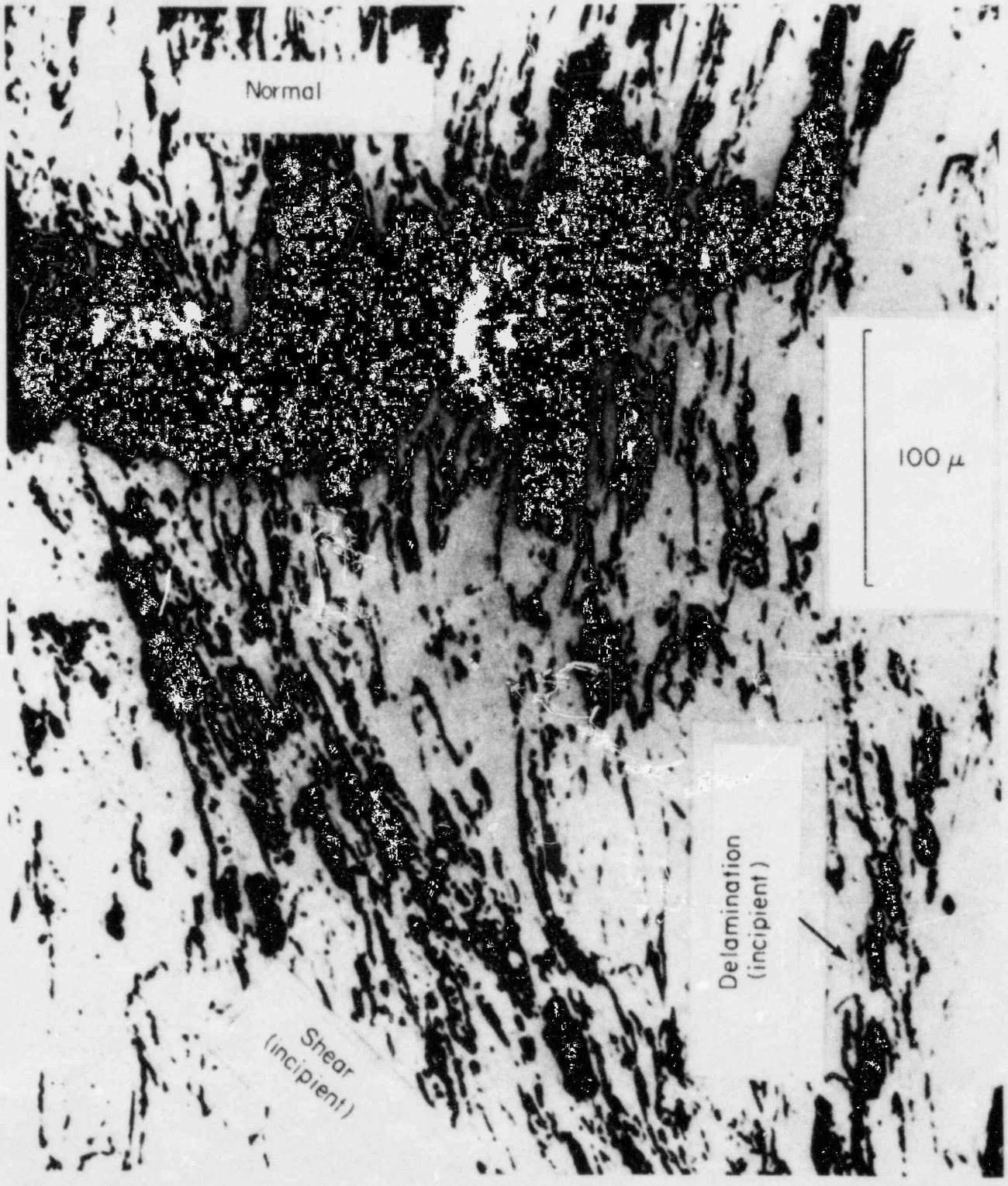

Fig. 3. Growing normal fracture and incipient delaminating and shear fractures in necked copper tensile specimen. Reprinted with permission from Fracture, F. A. McClintock, "Plastic Aspects of Fracture," copyright 1971, Academic Press.

plastic behavior of the material. The ultimate strength (σ_u) is the maximum engineering stress, after which the stress-strain curve for ductile material usually drops off to the point of fracture, which defines the maximum elongation (ε_f). Consequently, σ_u and ε_f represent two different points on the stress-strain curve. Because the point of ultimate strength really represents the point of maximum load, it is generally referred to as the point of mechanical instability. For primary loads, the structure will fail when the point of mechanical instability is exceeded.

In uniaxial tension experiments with ductile materials, there occurs a significant phenomenon that, within a small length of the specimen (much less than the gauge length), there is a drastic reduction of cross-section area after the point of ultimate strength is exceeded. The "necking" phenomenon may or may not be evident under combined-stress-state conditions. In the "neck" region, the stress and strain are much higher than the nominal (engineering) stress and strain. This fact, along with the argument that in the predominantly plastic region the material does not "remember" its original geometry, leads to a school of thought that advocates the use of current geometry for the prediction of failure for ductile materials. The stress and strain ($\bar{\sigma}$, $\bar{\varepsilon}$) referring to the current geometry are called the true stress and the true strain (or natural strain). The engineering stress and strain (σ, ε) refer to the original geometry. Figure 4 shows a comparison of the engineering and the true constitutive curves for AISI 1020 steel. The true stress-strain curve does not differentiate the constitutive relationship in compression and in tension. Referring to the tensile experiment, we may note that

1. at the point of mechanical instability, the true stress-strain curve does not have a zero slope, indicating that because of necking phenomena, the stress increases as the external load may remain constant;
2. as the post-stability deformation is mostly in the neck region, which is usually a fraction of the gauge length, the engineering stress-strain curve fails to show the real engineering strain in the neck region. The curve is dependent on the gauge length chosen.

Other proposed limit values include the maximum shearing strength (τ_u) resulting from torsion experiments and given in the engineering definition. Another is the uniform strain ($\bar{\varepsilon}_u$), which is the true strain at the start

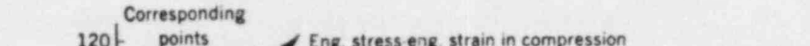

Fig. 4. Equivalent and engineering flow stress-strain curves in tension and compression for AISI 1020 steel, hot-rolled. Reprinted with permission from An Introduction to the Mechanics of Solids, S. H. Crandall and N. C. Dahl, copyright 1959, McGraw-Hill Book Co.[2]

of necking, corresponding to the ultimate strength point. Neither of these two limit values is commonly given material properties in the United States.

The analytical curve fitting of the stress-strain curve may be represented by several models including (a) the multilinear model, (b) the Ramberg-Osgood model, and (c) the extended Ramberg-Osgood model. The multilinear model is generally used in the updated Lagrangian formulation so that the stress-strain relation is linear within each analytical time step. The Ramberg-Osgood model assumes the approximation

$$\bar{\sigma} = A \bar{\varepsilon}^n , \tag{10}$$

where the exponent n ranges between 0.0 and 1.0. The model is not appropriate for regions where highly nonuniform stress fields exist. The extended Ramberg-Osgood model is a good approximation when the yield strain is small in comparison with the plastic strain; then

$$\bar{\sigma} - \sigma_y = A \bar{\varepsilon}^n . \tag{11}$$

In the Ramberg-Osgood model there is no yield stress but a very low 0.2% yield strength. The extended Ramberg-Osgood model is essentially a rigid-plastic approximation. Figures 5a and 5b show the Ramberg-Osgood approximations for AISI 1020 steel for different values of the exponent, n. Four curves are plotted in Fig. 5a using different values of the work-hardening exponent, n. All the curves have the single limiting point of 70% fracture strain, at a stress of 95 000 psi. The work-hardening exponent, n = 0.2, provides the best fit. In Fig. 5b, each curve with a different value of work-hardening exponent, n, is made to fit the corresponding stability point on the experimental stress/strain curve ($\varepsilon_u = n$). Again, n = 0.2 provides the best fit.

The extension of uniaxial experimental data to the fracture criterion of materials under triaxial states of stress is generally complicated. One method is the extension of the plastic-yielding theory with the use of the equivalent stress and the equivalent strain ($\bar{\sigma}_e$, $\bar{\varepsilon}_e$), where $\bar{\sigma}_e$ and $\bar{\varepsilon}_e$ are defined by Eqs. (8a) and (9a) respectively. The term "equivalent" indicates that the particular measure of stress and strain in the triaxial state of stress is equivalent to the stress and strain in the uniaxial experiment.

In the following paragraphs we discuss the theories of ductile fracture that have been proposed for use in evaluating CRBR response to accident loads.

1. The Maximum-Tensile-Stress Theory.

This oldest and simplest theory predicts cohesive failure of a material when the maximum principal stress (in tension) reaches the stress limit of the ultimate strength. Cohesive failure by high compressive loads, such as that in brittle fracture, is not considered for ductile fracture.

2. The Maximum-Shearing-Stress Theory

The basic philosophy of this theory is to extend Tresca's yield condition to that of fracture; the ultimate shearing strength is, therefore, the stress limit. Because information on the shearing strength is difficult to obtain, the stress limit can be approximated with the uniaxial experiment. For that case, the ultimate shearing strength is taken to be one-half of the ultimate strength. An alternate theory is to have the octahedral shearing stress reach a stress limit. It is observed that this theory extends the Hencky-Mises yield condition to fracture by allowing the equivalent stress to reach a limit equal to the ultimate strength. Generally, the stress limits of these theories are expressed as a function of the normal stresses on the corresponding shear planes.

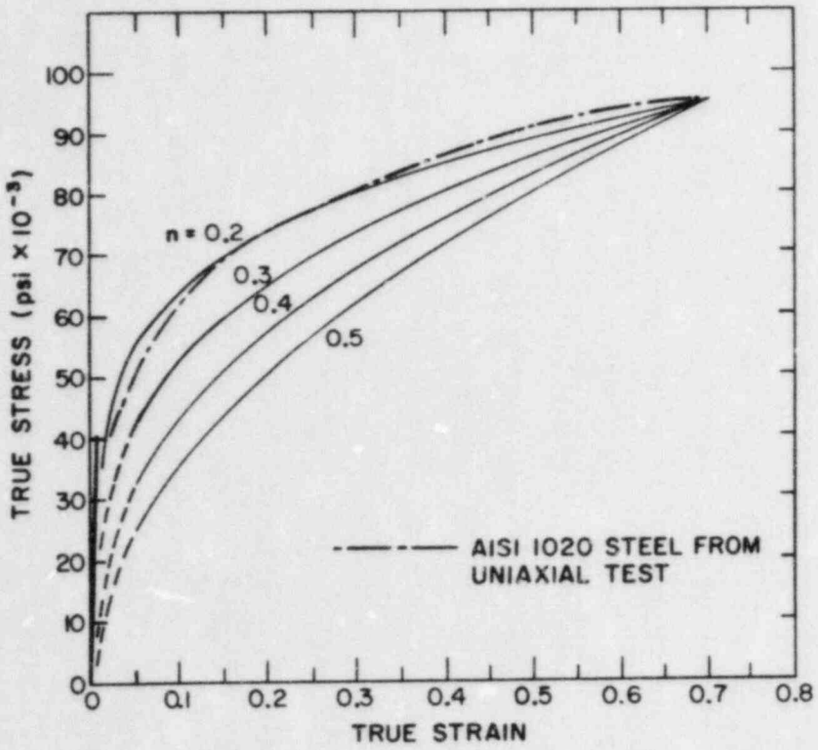

Fig. 5a. Ramberg-Osgood $\bar{\sigma}$ - $\bar{\varepsilon}$ curve ($\bar{\sigma} = A\bar{\varepsilon}^{n}$) based on maximum strain $\varepsilon_f = 0.7$ for AISI 1020 steel.

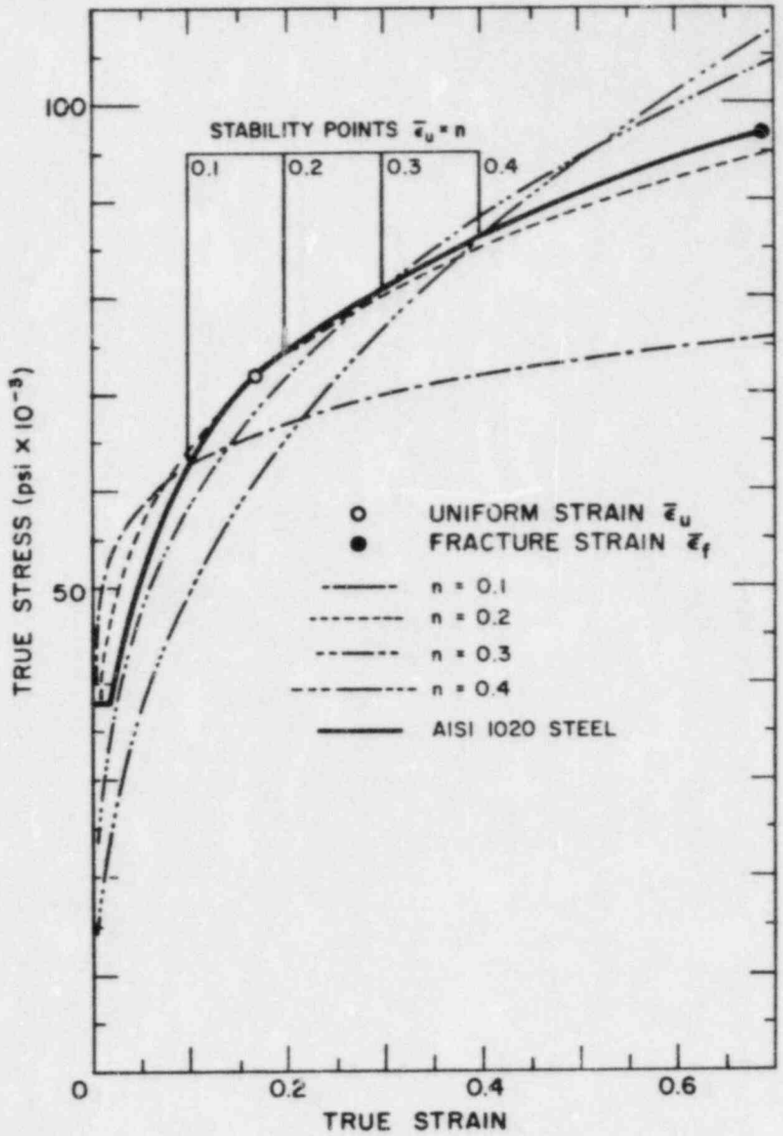

Fig. 5b. Ramberg-Osgood models ($\bar{\sigma} = A\bar{\varepsilon}^{n}$) for AISI 1020 steel for equal stability point.

3. The Maximum-Strain Theory

Under secondary stress, only the maximum strain (tensile) in a mechanical structure is limited to the maximum elongation ϵ_f. In view of many experiments showing reduced ϵ_f under combined stress states, a better proposal is to use the strain value at the onset of necking, ϵ_u or $\bar{\epsilon}_u$ (uniform strain), as the limiting value.

4. The Plastic-Instability Theory.

In uniaxial tensile experiments, the ultimate strength is reached at the onset of necking; the engineering stress is distinctly identifiable at the point that $d\sigma/d\epsilon = 0$ on the stress-strain curve. In the true stress-strain expression, the curve continues to rise after necking (Fig. 4). In that case, the point of plastic instability can be defined as the point of the maximum load,[3] or $dP = 0$. Hence, in terms of the current cross-sectional area A, $P = \bar{\sigma}A$, or $dP = \bar{\sigma}dA + Ad\,\bar{\sigma} = 0$, that is

$$\bar{\sigma}_u = - \left. \frac{Ad\bar{\sigma}}{dA} \right|_u \quad .$$

Assuming that up to the maximum strain the incompressibility condition of plasticity still holds, that is, $d(AL) = AdL + LdA = 0$,

$$\frac{dA}{A} = - \frac{dL}{L} = - d\bar{\epsilon} \quad .$$

We thus conclude that for the uniaxial state of stress, the plastic instability occurs when the ultimate true stress reaches a stress limit such that

$$\bar{\sigma}_u = \left[\frac{d\bar{\sigma}}{d\bar{\epsilon}} \right]_u \quad . \tag{12}$$

In a multiaxial stress state, we may extend Eq. (12) in terms of equivalent stress and strain (σ_e, ϵ_e) such that

$$\frac{\bar{\sigma}_e}{Z} = \frac{d\bar{\sigma}_e}{d\bar{\epsilon}_e} \quad \text{or} \quad \frac{1}{Z} = \frac{1}{\bar{\sigma}_e} \frac{d\bar{\sigma}_e}{d\bar{\epsilon}_e} \quad , \tag{13}$$

where Z is the subtangent as shown in Fig. 6.[4]

For uniaxial tension, the critical subtangent Z = 1. Hillier[4] developed a general expression for the critical subtangent as

$$\frac{1}{Z} = \frac{9}{4} \frac{1}{\bar{\sigma}_e^3} \sum_{\alpha} \left\{ \frac{1}{A_\alpha} \frac{\partial P_{\alpha j}}{\partial \bar{\varepsilon}_{mn}} \bar{s}_{mn} \bar{s}_{ij} \delta_{\alpha i} + \bar{\sigma}_{\alpha j} \bar{s}_{ij} \bar{s}_{\alpha\beta} \delta_{\alpha\beta} \delta_{\alpha i} \right\}, \quad (14)$$

where $\bar{\sigma}_{\alpha j}$ is the true stress tensor, $\bar{s}_{ij}$ is the deviatoric tensor of stress, and $P_{\alpha j}$ is the normal and shear component of force. Simplified equations were developed for plane strain, biaxial tension and shear in-plane stress, and thin tubes under internal pressure and axial load. No triaxial stress-state solution is available. McClintock[5] gave the results for internally pressurized, thin-wall spheres and thin-wall tubes. Hillier[6,7] compared his results with other theories for thin-wall tubes loaded by internal pressure and independent axial tension using both analytical and experimental data.

For cases where the critical subtangent Z can be computed and true stress-strain curves are available, the stress and strain limits ($\bar{\sigma}_\ell$, $\bar{\varepsilon}_\ell$) can be readily obtained at the tangent (Fig. 6). For some analyses, assuming the Ramberg-Osgood relationship, both Eqs. (10) and (13) simplify to

$$\bar{\varepsilon}_u = n \quad \text{and} \quad \bar{\varepsilon}_\ell = nZ \ . \quad (15)$$

Hence,

$$\bar{\varepsilon}_\ell = \bar{\varepsilon}_u Z \quad \text{and} \quad \bar{\sigma}_\ell = \bar{\sigma}_u Z^n \ . \quad (16)$$

Equations (15) and (16) do not hold for the extended Ramberg-Osgood relationship [Eq. (11)].

In its basic form, the plastic-instability theory is essentially a stress-limit theory.[4] It can be extended to determine the strain limit with an appropriate constitutive relationship such as Eq. (10).

5. The Hole-Growth Theory

Figure 3 shows evidence of the coalescence of holes with normal cracking; the incipient delamination actually shows the elliptical holes. Figure 7 shows

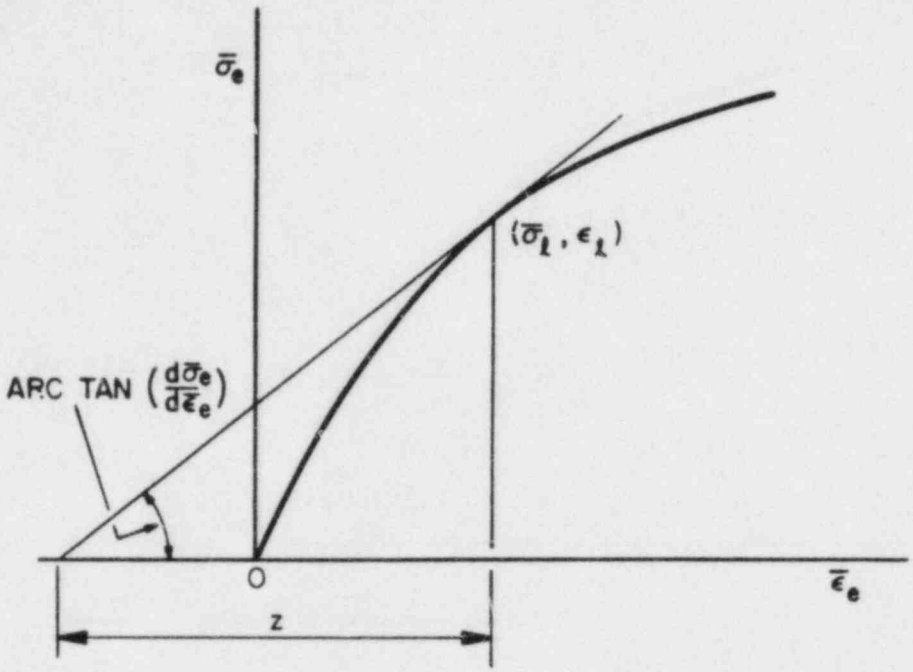

Fig. 6. Critical subtangent to the generalized strain-hardening curve.

in more detail the coalescence of holes in copper and plasticine. The mathematical theory of hole growth and subsequent coalescence was developed by McClintock.[8,9] He states: "The material is assumed to contain three mutually perpendicular sets of cylindrical holes of elliptical cross-section with axes parallel to the principal directions of the applied stress (and strain increments), Fig. 8.... The condition of fracture will be that the growth of the holes is such that ... one of the semiaxes a or b of the hole approaches half of the corresponding mean spacing, $\ell_a/2$ or $\ell_b/2$ respectively."[8]

A growth factor,

$$F_{zb} = (b/\ell_b)/(b^o/\ell_b^o) \ , \tag{17}$$

is introduced for which there exists a limit as a criterion for hole coalescence. Because fracture occurs when F_{ij} reaches a critical value F_{ij}^f, the damage is then defined as $dn_{ij} = d(\ln F_{ij})/(\ln F_{ij}^f)$. The fracture strain is derived as

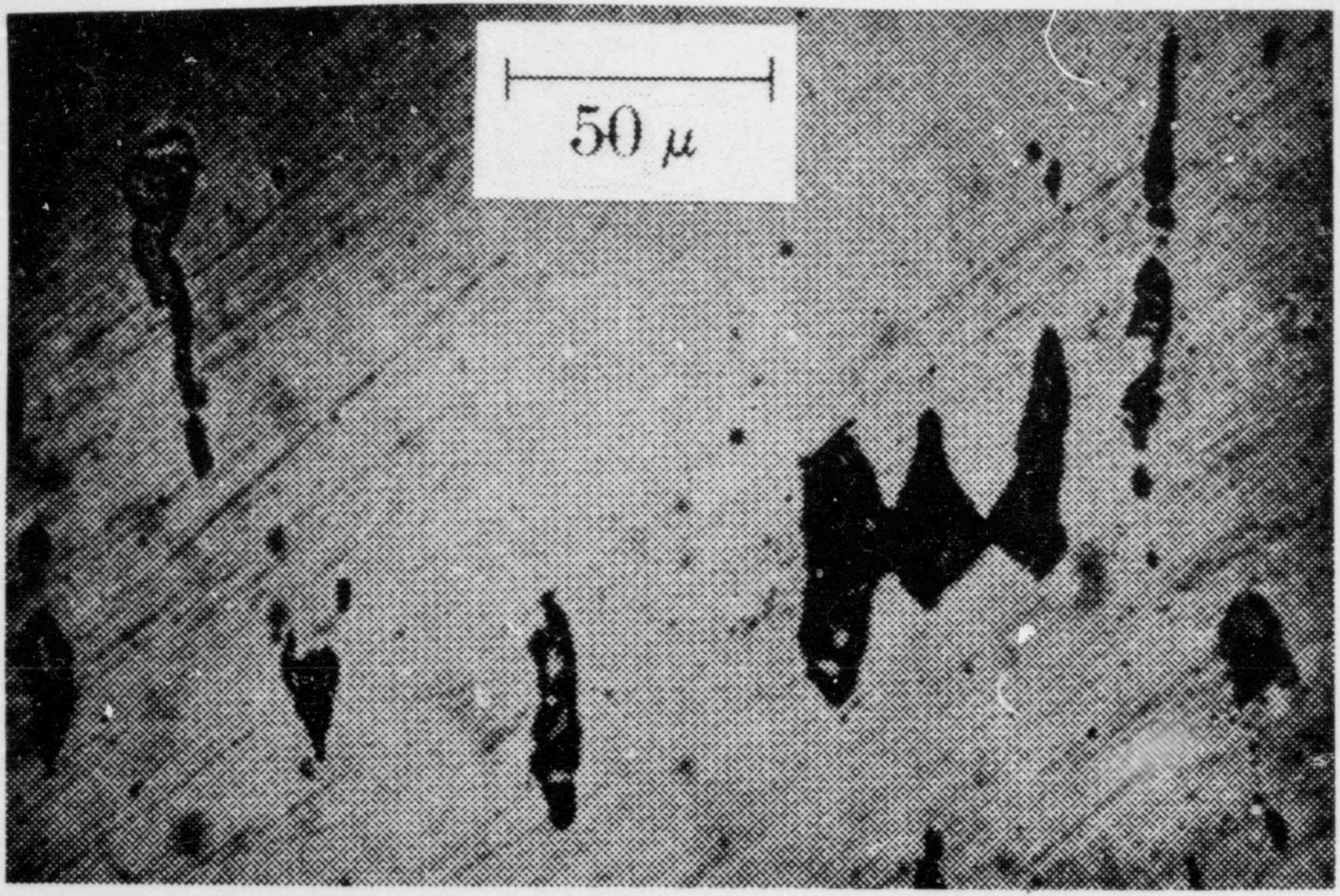

Fig. 7. Coalescence of holes. McClintock (1968). Reprinted with permission from Journal of Applied Mechanics, F. A. McClintock, "A Criterion for Ductile Fracture by the Growth of Holes," copyright 1968, American Society of Mechanical Engineers.

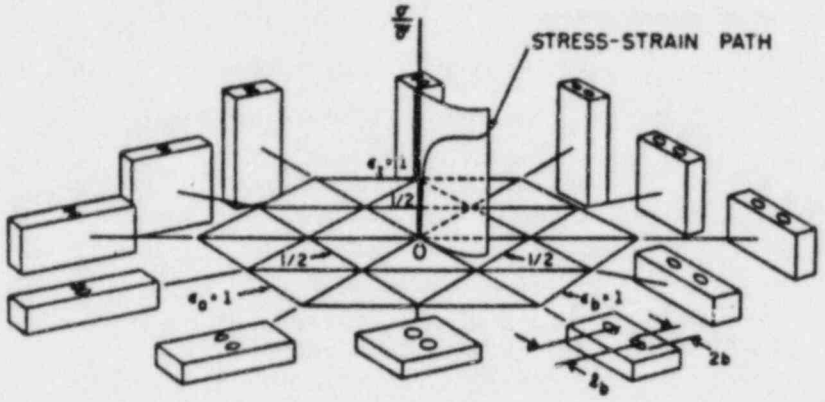

Fig. 8. Strain plane with corresponding deformations of a cube containing two holes coalescing in the b direction. Reprinted with permission from Journal of Applied Mechanics, F. A. McClintock, "A Criterion for Ductile Fracture by the Growth of Holes," copyright 1968, American Society of Mechanical Engineers.

$$\bar{\varepsilon}^f = \ln F^f_{zb} \Big/ \left[\frac{\sqrt{3}}{2(1-n)} \sinh \left(\frac{\sqrt{3}(1-n)}{2} \frac{\bar{\sigma}_a + \bar{\sigma}_b}{\bar{\sigma}_e} + \frac{3}{4} \frac{\bar{\sigma}_a - \bar{\sigma}_b}{\bar{\sigma}_e} \right) \right], \qquad (18)$$

when n is the strain-hardening coefficient that may either be the exponent in the Ramberg-Osgood relationship [Eq. (10)] or be defined in terms of the stress at the point of uniform strain divided by the average stress over the stress-strain curve up to the uniform strain, that is

$$n = [\bar{\sigma}_u / \bar{\sigma}_{\text{avg to } \bar{\varepsilon}_u}] - 1 \quad . \qquad (19)$$

The expression in Eq. (18) may be approximately simplified for cases of plane tension to

$$\bar{\varepsilon}^f = (1-n) \ln F^f_{zb} \Big/ \sinh \left[\frac{\sqrt{3}}{2} (1-n) \frac{\bar{\sigma}_a + \bar{\sigma}_b}{\bar{\sigma}_e} \right] \quad . \qquad (20)$$

McClintock considered that the expression in Eq. (20) is good to 15% at high triaxiality, where the triaxiality (TF) is defined as $TF = (\bar{\sigma}_a + \bar{\sigma}_b + \bar{\sigma}_c)/\bar{\sigma}_e$. At low triaxiality it may differ from Eq. (18) by a factor of two. For instance, in uniaxial tension Eq. (18) yields a fracture strain of $0.64356(\ell n F^f_{zb})$, whereas Eq. (20) gives $1.07733\ (\ell n F^f_{zb})$, both using n = 0.25.

Using an order of magnitude estimate, McClintock derived for ellipsoidal holes for triaxial state of stress

$$\bar{\varepsilon}^f = \frac{1}{3}(1-n)\ \ell n\ F^f_{ij} \Big/ \sinh\left[\frac{\sqrt{3}}{3}\ (1-n)\ TF\right] \qquad (21)$$

McClintock indicates that there is good correlation for aluminum, but the hole-growth theory overestimates fracture strain for copper-dispersion alloys (see Fig. 9).[9,10]

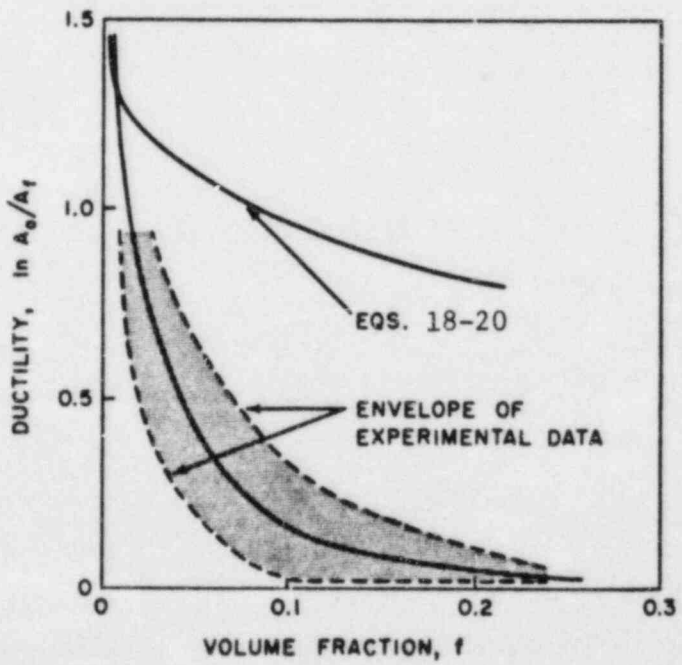

Fig. 9. Comparison of ductility of copper-dispersion alloys with hole-growth theory. Reprinted with permission from Ductility, F. A. McClintock, "On the Mechanics of Fracture from Inclusions," copyright 1968, American Society for Metals.

V. GENERAL REVIEW

For ductile fracture many diversified theories are being proposed. There is the basic question of whether material properties generated from the uniaxial tension test are representative of the ductile failure for other stress states. We must also question whether the point of mechanical instability or the point of fracture is to be used as the limit point. According to the ASME code, Section III, Appendix F, for Level D primary loading,[11] the maximum load is to be 70% of the mechanical instability load. The criterion leaves an extensive region past the stability point as available fracture toughness in fracture design. The following review will address the merits and shortcomings of individual theories.

The stress criteria are simple to use and need not be converted to the true stress form in the elementary applications of the maximum stress theory and the maximum shearing stress theory. One form or another of the theory is popularly used in numerical computations as a criterion for fracture initiation. Typical examples are the maximum tensile stress as a criterion for the initiation of mode I cracks, and the maximum octahedral shearing stress (equivalent to the so called "von Mises" stress) for the initiation of mode II or mode III cracks. These criteria are applicable for uniaxial tension or simple shear states of stress. For complex states of stress both theories have been disproved by Bridgeman's experiments performed during World War II. An updated discussion can be found in Nadia.[12] Bridgeman's experiments involved small cylindrical bar specimens, to each of which a constant high fluid pressure p was superimposed while the specimen was stretched in tension. States of stress at the center of the break section and at surface of the neck are shown in Mohr's diagrams for four pressure levels as reproduced from Nadia[12] in Fig. 10. Bridgeman himself proposed the mean stress as a criterion but the proposal is readily disproved with a specimen failure in pure shear for which the mean stress is zero.

It is therefore concluded that a single stress limit alone is not adequate to define fracture initiation. If the stress limit is to be established other parameters may have to be taken into account. One of such proposal is similar to the Mohr's theory of failure that there exists an envelope curve in the stress plane to the Mohr's circles, such as that in Fig. 10b and Fig. 1. The circle that is tangent to the envelope is the limiting state of stress. The

theory seems to work best with dominant shear failure, and Fig. 11 shows an increasing fracture stress with increasing lateral pressure to the cylinder. The experiments constitute a good counter example for cohesive failure.

The theoretically sound stress-limit criterion is the plastic-instability theory, Eq. (13). It is, however, pointed out by Hillier[6] that the theory predicts the point of instability rather than the fracture point; experiments

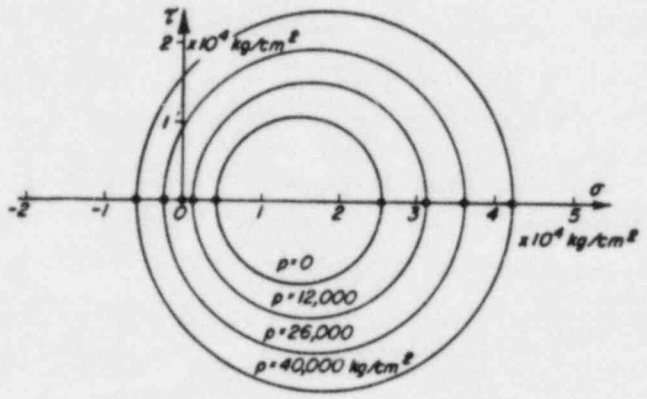

Fig. 10a. Stresses at center of minimum cross sections.

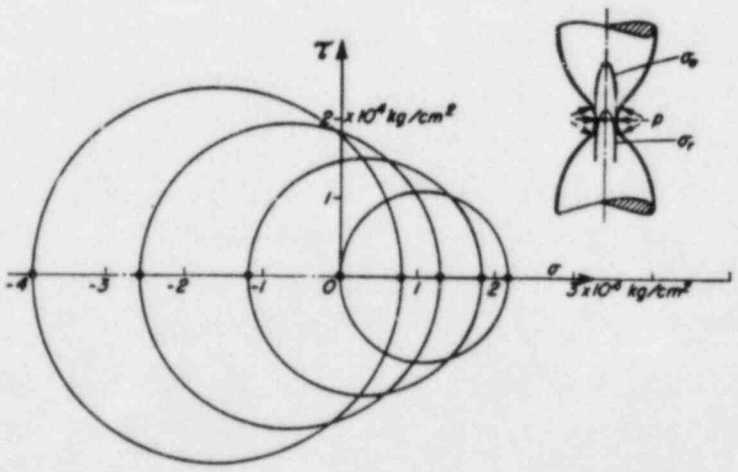

Fig. 10b. Stresses at surface of neck (r = a).

Fig. 10. The major principal stress circles representing the stresses at fracture in Bridgman's tension tests for steel bars exposed simultaneously to high hydrostatic pressure p. Reprinted with permission from Theory of Flow and Fracture of Solids, A. Nadia, copyright 1950, McGraw-Hill Book Co.

on failure usually lead to fracture instead of the instability point. Consequently, the theory is at best verified qualitatively, and controlled stability experiments are still much needed. However, when the stress state is caused by primary loads, the mechanical structure will, theoretically, continue its deformation to fracture once the stability point is passed. Hence, for conservative design, the plastic-instability criterion is recommended for all primary stress states.

The simple strain-limit theory suffers the same problem of oversimplification, regardless of whether the fracture strain or the uniform strain is being used. That the limit is affected by the state of stress (or triaxiality factor, TF), was demonstrated by Bridgman's experiments with two types of steel; results are shown in Fig. 11, which is reproduced from Ductility.[13] Furthermore, the limiting strain value is very sensitive to the gauge length used in either the experiment or the numerical analysis. Figure 12 shows various strain paths and fracture points corresponding to different gauge lengths. A workable strain-limit theory, therefore, must also take other factors into consideration.

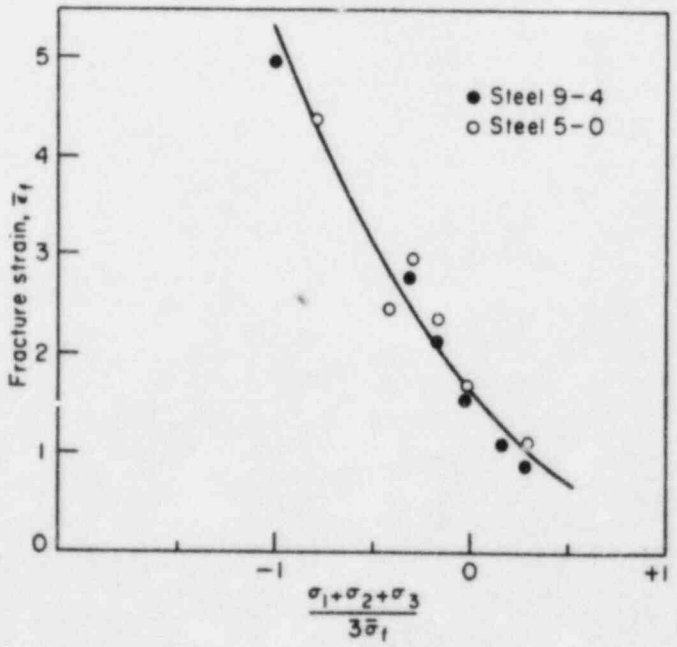

Fig. 11. Correlation between fracture strain and ratio of hydrostatic pressure to effective stress at fracture. Reprinted with permission from Ductility, G. E. Dieter, "Introduction to Ductility," copyright 1968, American Society for Metals.

The hole-growth theory, dealing with the changing geometry of the hole, is a natural extension of the strain-limit theory. The fracture strain given in Eq. (18) was developed by plasticity analysis for a planar tension field; however, in most applications the simpler Eq. (20) has been used, including its extension to the three-dimensional expression. Figure 13, which plots the damage ($\varepsilon_f / \ell n F^f_{zb}$) as a function of triaxiality factor, illustrates the difference between the two equations using a work-hardening exponent of n = 0.2. Up to a triaxiality factor (TF) of 1.85, Eq. (20) yields a higher fracture-strain limit than that of Eq. (18), which is by no means conservative. Only for a TF > 1.85 does the approximate Eq. (20) yield lower fracture strains as limit values than those predicted by the analytical Eq. (18). Users of the approximate equation should be aware of this fact. Because the simplified Eq. (20) is generally used, further comparison would help decide the level of conservatism of a criterion. We shall construct the ratio of triaxial fracture strain to the uniaxial fracture strain ($\varepsilon_f / \varepsilon_{fu}$). The analytical fracture strain Eq. (18) yields

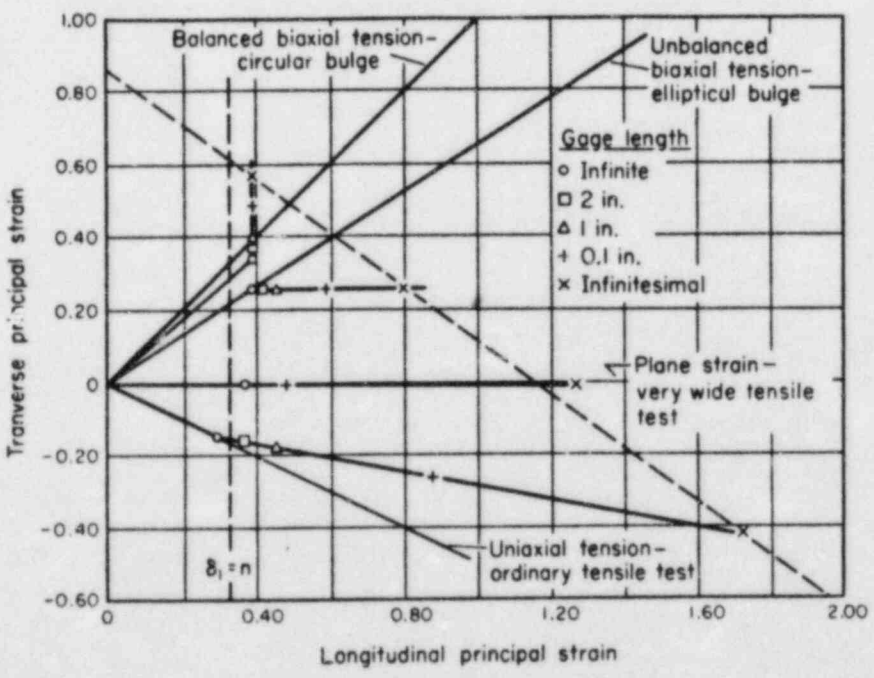

Fig. 12. Effect of biaxial stress state on ductility of sheet steel. Reprinted with permission from Ductility, G. E. Dieter, "Introduction to Ductility," copyright 1968, American Society for Metals.

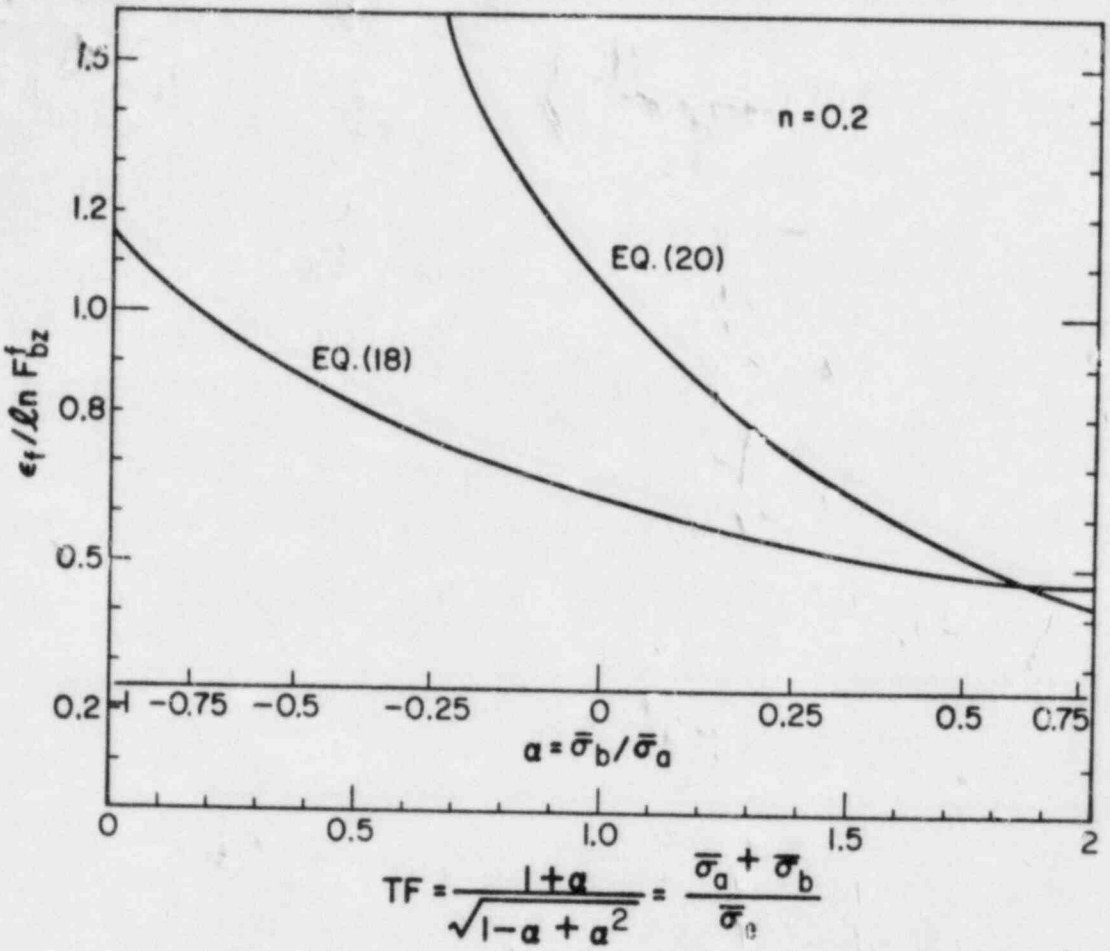

Fig. 13. Comparison of damage for exact and approximate equations of hole-growth theory.

$$\frac{\bar{\epsilon}_f}{\bar{\epsilon}_{fu}} = \frac{\left[\frac{\sqrt{3}}{2(1-n)} \sinh\left(\frac{\sqrt{3}}{2}(1-n)\right) + \frac{3}{4}\right]}{\left[\frac{\sqrt{3}}{2(1-n)} \sinh\left(\frac{\sqrt{3}}{2}(1-n)\,TF\right) + \frac{3}{4}\,\frac{1-\alpha}{\sqrt{1-\alpha+\alpha^2}}\right]}, \tag{22}$$

where $\alpha = \bar{\sigma}_b / \bar{\sigma}_{ai}$, whereas the simplified expression Eq. (20) leads to

$$\frac{\bar{\epsilon}_f}{\bar{\epsilon}_{fu}} = \sinh\left(\frac{\sqrt{3}}{2}(1-n)\right) / \sinh\left(\frac{\sqrt{3}}{2}(1-n)\,TF\right) . \tag{23}$$

Figure 14 plots both against the triaxiality factor, TF. One criterion proposed by Westinghouse* is to let the true maximum positive principal strain from multiaxial loading have a maximum value of 70% of uniaxial true fracture strain as shown in Fig. 15. The proposed limit would be conservative only if the material fractures under a triaxial state of stress with TF $\geq$ 1. There are many uncertainties associated with the theory that have yet to be resolved. These include the assumptions on the proportional increase of stress and the coincidence of major and minor axes of the eliptical hole with the principal axes of stress. The overestimate on some experiments as described below has yet to be explained. Furthermore, the analytical development of the hole-growth theory assumes no anisotropy and is based on a proportional biaxial tensile stress field. Its extension to the shear band has yet to be derived

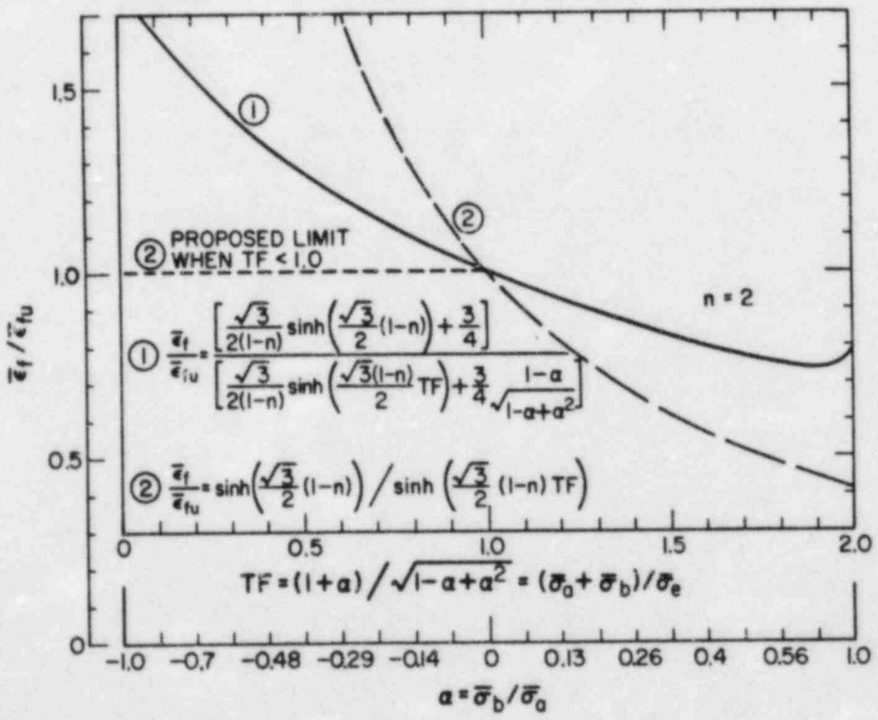

Fig. 14. Fracture strain as a function of triaxiality factor.

*Information provided by the Westinghouse Electric Corporation, Advanced Reactor Division, Madison, Pennsylvania 15663.

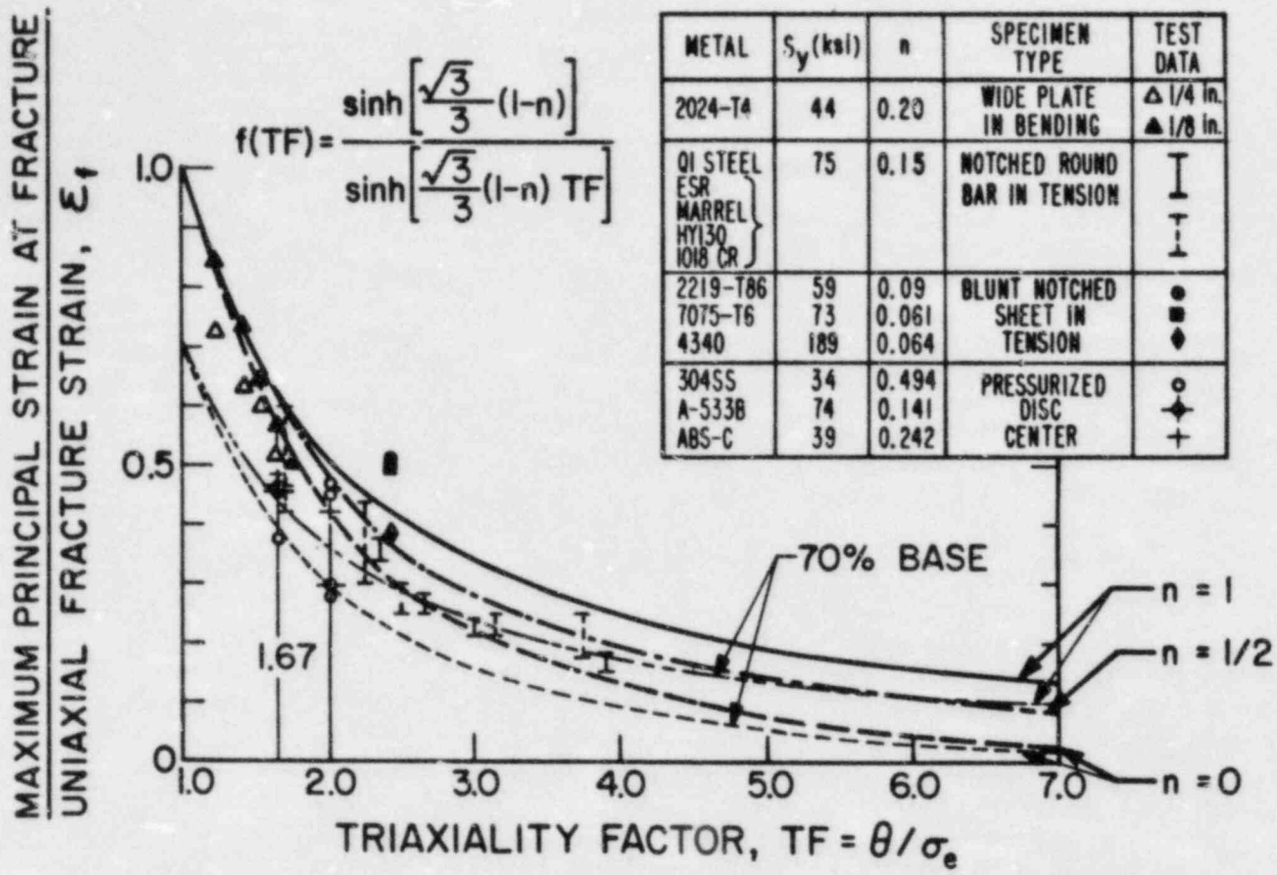

Fig. 15. Fracture criterion proposed by Westinghouse.*

analytically from plasticity theory.[14] The lack of theoretical justification may have accounted for some disturbing experimental results. For instance, the hole-growth theory would predict a higher fracture strain in shear (TF = 0) than that of uniaxial tension (TF = 1), even though experiments on some materials have proved otherwise as shown in Table I (McClintock[9]). Of the eight materials tested, six show the ratio ($\varepsilon_f/\varepsilon_{fu}$) less than 1 at TF = 0. The data submitted by Westinghouse* cover only the region for TF > 1.0 (Fig. 15). In Fig. 15, a 70% base is drawn as a limit, which is adequate for TF > 2.0. For TF $\leq$ 2.0, even a 70% base is marginal.

It is therefore concluded that for high TF (greater than 2.0), the criterion based on the hole-growth theory may be adopted. For low TF, the

*Information provided by the Westinghouse Electric Corporation, Advanced Reactor Division, Madison, Pennsylvania 15663.

TABLE I

COMPARISON OF FRACTURE STRAIN IN TENSION AND TORSION[a]

Material	Tensile Strength (psi)	True Fracture (Tension)	Equivalent Plastic Strain (Torsion)
1100-0 aluminum, annealed 660°F	13,000	2.62	7.3
60-40 brass, as-rolled	56,000	0.68	0.51
7075-T6 aluminum alloy	84,000	0.37	0.34
7075-T6 aluminum alloy	84,000	0.44	0.48
1045 steel, 1575°F;[b] Oil quench temp 400°F	271,000	0.52	0.16
1045 steel, 1575°F;[b] Water quench temp 800°F	R_C40[c] (188,000)	0.88	0.39
1045 steel, 1575°F;[b] Salt quench temp 800°F	R_B92[c] (80,000)	0.93	0.38
1045 steel, 1575°F;[b] Salt quench temp 1100°F	R_B86[c] (62,000)	0.89	0.43

[a] Table adapted from Ref. 11.
[b] Material heated to 1575°C, then quenched as noted.
[c] Rockwell hardness (B or C scale)

hole-growth theory fails to relate the failure phenomenon physically. More controlled experiments in that range are necessary to establish a rigorous criterion.

In conclusion, it is recommended that

1. for yield, the Hencky-Mises criterion, Eq. (2), is to be used. Its simplified and other alternate forms [Eqs. (4), (7a)] may be used if the yield function, f(p), is not available;

2. the triaxiality factor be used as a single, deciding parameter in ductile fracture. The work-hardening exponent should be determined by the mechanical instability point, Fig. 5b, because higher values generally result in stiffer plastic constitution, leading to underestimation of deformation. It seems safe to use the criterion based on the hole-growth theory in the range of TF $\geq$ 2, for steel-based ductile metals;
3. for TF $\leq$ 1, use the ASME existing code,[11] a conservative (perhaps overly so) but safe criterion, until more experimental data become available to substantiate other criteria;
4. in the range 1 $\leq$ TF $\leq$ 2, data in Fig. 15 tend to indicate marginal conservatism. However, a 70% baseline is considered adequate for evaluation of accidents beyond the design base;
5. as shown in Fig. 15, the use of the uniform strain as a limit is generally considered to be conservative for low triaxiality (TF < 2.5). The failure criterion, however, is not yet verified by experiments for TF < 1. It is strongly recommended that controlled experiments be conducted for the materials of interest to fill such a vacuum;
6. all computed strains to be compared with the strain limit should be the mechanical strains corresponding to the stress state on the given stress-strain curve. In thermal stress analysis, the actual strain consists of the thermal strain and the mechanical strain. For a lineal member constrained at both ends, heated to have a temperature rise of ΔT, the actual strain ε_A (being constrained) is zero. The thermal strain is $\varepsilon_T = \alpha\Delta T$; the corresponding mechanical strain ε_M is therefore

$$\varepsilon_M = \varepsilon_A - \varepsilon_T = -\alpha\,\Delta T \ .$$

REFERENCES

1. F. A. McClintock and A. S. Argon, Mechanical Behavior of Materials, (Addison-Wesley, Reading, Mass., 1966).
2. S. H. Crandall and N. C. Dahl, An Introduction to the Mechanics of Solids (McGraw-Hill, New York, 1959).

3. American Society of Mechanical Engineers Boiler and Pressure Vessel Code, Sec. III, Div. 2, Article F-1321.1(e) (1980).

4. M. J. Hillier, "Tensile Plastic Instability Under Complex Stress," Int. J. Mech. Sci. 5, 57-67 (1963).

5. F. A. McClintock and A. S. Argon, Mechanical Behavior of Materials (Addison-Wesley, Reading, Mass. 1966).

6. M. J. Hillier, "Tensile Plastic Instability of Thin Tubes-I," Int. J. Mech. Sci. 7, 531-538 (1965).

7. M. J. Hillier, "Tensile Plastic Instability of Thin Tubes - II," Int. J. Mech. Sci. 7, 539-549 (1965).

8. F. A. McClintock, "A Criterion for Ductile Fracture by the Growth of Holes," J. Appl. Mech. 35, 363-371 (1968).

9. F. A. McClintock, "Plastic Aspects of Fracture," in Fracture, H. Liebowitz, Ed. (Academic Press, New York, 1971), Vol. III, Chap. 2, pp. 79-98.

10. F. A. McClintock, "On the Mechanics of Fracture from Inclusions," in Ductility (Amer. Soc. Metals, Metals Park, OH, 1968), Chap. 9, pp. 266-270.

11. American Society of Mechanical Engineers Boiler and Pressure Vessel Code, Sec. III, Div. 2, Articles F-1324.4, F-1324.5 (1980).

12. A. Nadia, Theory of Flow and Fracture of Solids, 2nd ed. (McGraw-Hill, New York, 1950), Vol. 1, Chap. 17, pp. 271-274.

13. G. E. Dieter, "Introduction to Ductility," in Ductility (Amer. Soc. Metals, Metals Park, OH, 1968), Chap. 1, pp. 1-30.

14. F. A. McClintock, S. M. Kaplan, and C. A. Berg, "Ductile Fracture by Hole Growth in Shear Bands," Int. J. Frac. Mech. 2, 614-627 (1966).

DISTRIBUTION

	Copies
Nuclear Regulatory Commission, R7, Bethesda, Maryland	248
Technical Information Center, Oak Ridge, Tennessee	2
Los Alamos National Laboratory, Los Alamos, New Mexico	50
	300

NRC FORM 335 (6-83) U.S. NUCLEAR REGULATORY COMMISSION

BIBLIOGRAPHIC DATA SHEET

1 REPORT NUMBER (Assigned by TIDC, add Vol. No., if any)
NUREG/CR-3644
LA-10007-MS

2 Leave blank

3 TITLE AND SUBTITLE
Review of Proposed Failure Criteria for Ductile Materials

4 RECIPIENT'S ACCESSION NUMBER

5 DATE REPORT COMPLETED
MONTH: January YEAR: 1984

6 AUTHOR(S)
Frederick D. Ju, Thomas A. Butler

7 DATE REPORT ISSUED
MONTH: April YEAR: 1984

8 PERFORMING ORGANIZATION NAME AND MAILING ADDRESS (Include Zip Code)
Los Alamos National Laboratory
Los Alamos, New Mexico 87545

9 PROJECT/TASK/WORK UNIT NUMBER

10 FIN NUMBER
A7270

11 SPONSORING ORGANIZATION NAME AND MAILING ADDRESS (Include Zip Code)
Clinch River Breeder Reactor Program Office
Office of Nuclear Reactor Regulation
US Nuclear Regulatory Commission
Washington, DC 20555

12a TYPE OF REPORT
Technical

12b PERIOD COVERED (Inclusive dates)

13 SUPPLEMENTARY NOTES

14 ABSTRACT (200 words or less)

In this report, failure criteria for structural components constituting the primary coolant-system boundary of a Liquid Metal Fast Breeder Reactor (LMFBR) are reviewed. Because the materials being considered, mild ferritic steel and austenitic stainless steels, are ductile, especially under LMFBR normal operating and accident conditions, only ductile criteria are considered. The ductile criteria must be used in combination with true stress and strain measures of deformation and internal load. Specific criteria reviewed include maximum stress and strain or plastic instability based on uniaxial tensile-test data and a hole-growth theory based on coalescence of neighboring voids under load. Criteria based only on maximum stress or strain are not recommended for general use because they are not appropriate under general multiaxial stress conditions. The plastic instability criterion, because it leaves a large unused toughness region before fracture, is recommended where considerable conservatism is warranted. The hole-growth criterion is recognized as being analytically sound; however, it has not been extended to general three-dimensional geometry and multiaxial stress conditions. The theory needs to be substantiated with experimental data for specific materials being considered.

15a KEY WORDS AND DOCUMENT ANALYSIS

15b DESCRIPTORS

16 AVAILABILITY STATEMENT
Unlimited

17 SECURITY CLASSIFICATION (This report)
Unclassified

18 NUMBER OF PAGES

19 SECURITY CLASSIFICATION (This page)
Unclassified

20 PRICE
$